An experimental study of HF photodissociation: Spin–orbit branching ratio and infrared alignment

J. Zhang, C. W. Riehn, M. Dulligan, and C. Wittig
Department of Chemistry, University of Southern California, Los Angeles, California 90089-0482

(Received 22 December 1995; accepted 23 January 1996)

Single rotational levels of HF ($v=3$) were prepared by using overtone excitation and these molecules were then photodissociated by ultraviolet (UV) radiation at 193.3 nm. Time-of-flight spectra of the hydrogen atom fragment provided the spin–orbit state distribution of the fluorine fragment. Changing the UV photolysis laser polarization confirmed an $A\ ^1\Pi \leftarrow X\ ^1\Sigma^+$ electronic transition in the photodissociation step. Photodissociation of HF at 121.6 nm is also reported. Infrared (IR) induced alignment of the diatom was studied by monitoring the IR laser polarization dependence of the H-atom product angular distribution. Depolarization due to hyperfine interaction was studied by using the $R(0)$ transition. Agreement with theory is excellent. © *1996 American Institute of Physics.* [S0021-9606(96)03216-5]

I. INTRODUCTION

Hydrogen halides are among the simplest model systems for studying photophysics and photochemistry.[1–17] Their lowest energy UV absorption bands are assigned to a $\sigma^* \leftarrow np\pi$ transition, and dissociation into atomic fragments $H(^2S)$ and $X(^2P)$ occurs with the spin–orbit electronic excitation of the halogen atom as the only internal energy, aside from the hydrogen and halogen hyperfine levels.

Four electronic surfaces ($^1\Sigma^+$, $^3\Sigma^+$, $^1\Pi$, and $^3\Pi$) correlate with $H(^2S)+X(^2P)$. The $X\ ^1\Sigma^+$ state is the ground state, and among the upper repulsive states, $^1\Pi$ and $^3\Pi$ originate from the $\sigma^* \leftarrow np\pi$ transitions, while $^3\Sigma^+$ can be accessed via a $\sigma^* \leftarrow \sigma$ transition at higher energy. Though photoexcitation often promotes HX molecules—especially those with lighter atoms, such as HF and HCl—to a single electronic surface, nonadiabatic couplings between excited surfaces can redistribute the photodissociation flux. The multiple-surface environment of the excited states provides a means for studying nonadiabatic couplings between excited electronic states. A strong indication of such coupling can be observed via the spin–orbit branching ratio, and its measurement may provide insight into mechanisms. Furthermore, theoretical calculations on hydrogen halides are tractable because of their simple nature.[1,8–11,17]

The photochemistries of HCl, HBr, and HI have been studied extensively.[1–17] The spin–orbit branching ratio from photodissociation of HCl in the ground vibrational state has been investigated both experimentally and theoretically. The measured ratio $[Cl(^2P_{1/2})]/[Cl(^2P_{3/2})]$ was found to be 0.50 ± 0.05 at 193.3 nm and 0.88 ± 0.13 at 157 nm,[2–6] and it was shown for these wavelengths that the electronic transition is primarily perpendicular ($A\ ^1\Pi \leftarrow X\ ^1\Sigma^+$).[2–6] Very recently, the ratio has been measured between 193.3 and 119.3 nm.[7] Givertz *et al.*[8] and Alexander *et al.*[9] used *ab initio* methods to calculate the branching ratio; however, the results differ from each other, as well as from the early experimental data.[6,9] The discrepancies prompted two further theoretical studies,[10,11] and it was shown that the branching ratio is very sensitive to details of the nonadiabatic coupling. The most recent experimental data are in reasonable agreement with the calculations of Alexander *et al.*[7,9] Further experimental and theoretical studies of the HCl system are necessary to fully understand this coupling. Photodissociation of HBr in the ground vibrational state was also studied at various wavelengths. The branching ratio $[Br(^2P_{1/2})]/[Br(^2P_{3/2})]$ was measured to be 0.12 and 0.16 at 243 and 193.3 nm, respectively.[4,12,13] At 243 nm the Br* channel arises from a parallel transition and the Br channel corresponds to a perpendicular transition.[13] In contrast, at 193.3 nm both channels originate primarily from a perpendicular transition.[12] Of all the hydrogen halides, photodissociation of HI has been studied most thoroughly, at least experimentally.[12,14–17] The branching ratio $[I(^2P_{1/2})]/[I(^2P_{3/2})]$ has been measured[12,14–16] and calculated[17] at various wavelengths between 266 and 193.3 nm, and it has been found to vary dramatically, exhibiting values as low as ~0.1 and as high as ~1.5. The I and I* channels are shown to originate primarily from perpendicular and parallel transitions, respectively. Photodissociation of HI is influenced by strong spin–orbit interaction in the I atom; in addition to the zeroth-order singlet surfaces, zeroth-order triplet states are involved in the electronic transitions, which is not the case for HF and HCl.

Only a few studies regarding the photodissociation of vibrationally excited hydrogen halides have been reported. Photodissociation of vibrationally excited HBr was examined by Zittel and Little,[18] in which IR laser excitation prepared the diatom in $v=1$. Dissociation was induced by subsequent UV laser excitation. The absorption cross section of HBr ($v=1$) at 259 nm was measured by using mass spectrometry, but no detailed studies of the photodissociation dynamics such as product branching ratio and angular distribution were carried out. Theoretical calculations have been performed for the dissociation of vibrationally excited HCl,[8,10] and these studies predict an energy dependence on the branching ratio. Measurement of the ratio would be a sensitive probe for investigating nonadiabatic couplings. It was suggested from a theoretical investigation of vibra-

tionally excited HI that the I*/I branching ratio can be controlled through vibrational excitation.[19]

HF absorption lies in the VUV, starting at ~150 nm and peaking near 120 nm.[20,21] Theoretical studies suggest that this broad feature corresponds to the $A\ ^1\Pi \leftarrow X\ ^1\Sigma^+$ electronic transition.[22–26] Since HF absorbs only in the VUV, little of its photophysics has been examined. Because vibrational excitation extends the absorption to longer wavelengths, HF photodissociation dynamics may be investigated by using an IR+UV photolysis scheme. In the present study, HF was excited to a single rotational level in the $v=3$ vibrational state by using intense, narrow-linewidth IR radiation and these excited molecules were then photodissociated by using UV radiation at 193.3 nm. Hydrogen atom product TOF spectra were recorded by using the high-*n* Rydberg time-of-flight (HRTOF) technique. We also examined photodissociation of HF at 121.6 nm, which is near the absorption maximum.

In addition to imparting vibrational excitation, the IR radiation aligns the sample.[27–29] Specifically, for a rigid diatom like HF, the probability of aligning the rotational level J by excitation with linearly polarized light is given by[27]

$$P_J(\theta)=\frac{1}{4\pi}\left[1+A_0(J)P_2(\cos\ \theta)\right], \tag{1}$$

where θ is the angle between the molecular axis and the electric vector of the polarized radiation, and $P_2(\cos\ \theta)$ is the second-order Lengendre polynomial. $A_0(J)$ is the alignment parameter, which ranges from $+2$ for $P_J(\theta)\propto\cos^2\theta$ to -1 for $P_J(\theta)\propto\sin^2\theta$. $A_0(J)=0$ for an isotropic distribution. For R-branch transitions ($J=J''+1$), the alignment parameter is $A_0^R(J'')=(J''+2)/(2J''+1)$,[27] yielding $A_0(J)$ values of 2 and 1 for $R(0)$ and $R(1)$ transitions, respectively. For P-branch transitions ($J=J''-1$), $A_0^P(J'')=(J''-1)/(2J''+1)$.[27] For $P(1)$, $A_0^P(1)=0$ and $P_J(\theta)$ is isotropic. In the high J'' limit, $A_0^R(J'')$ and $A_0^P(J'')$ both converge to the asymptotic value of 0.5.

The above-mentioned alignment is brought about by absorption of linearly polarized light. However, samples thus aligned undergo depolarization due to the coupling of the molecular rotational angular momentum (in this case=**J**) to the nuclear spin **I** (hyperfine coupling).[28,30–35] Specifically, though **J** can be aligned by the absorption of radiation, the hyperfine splittings lie within the laser linewidth. Consequently, randomly distributed nuclear spins will couple to **J** after optical excitation and reduce the degree of alignment. This is referred to as depolarization. For closed-shell HF, only depolarization due to hyperfine coupling must be considered, and this has been studied theoretically by Altkorn *et al.*,[33] and can be described by a time-dependent depolarization coefficient $G^{(k)}(t)$, where k is the order of orientation ($k=1$) and alignment ($k=2$) parameters. The alignment parameter evolves in time according to

$$A_0(t)=A_0(t=0)G^{(2)}(t). \tag{2}$$

The depolarization coefficient was calculated for HF($v=1$) with $J=1$–3, 10. It displayed hyperfine quantum beats with ~μs recurrence times. Recently Orr–Ewing *et al.* investigated the time dependence of HCl($v=1, J$) alignment.[35] Linearly polarized IR radiation aligned the HCl molecule in the $v=1$, $J=1$ state, and the time dependence of the alignment was monitored by subsequent (2+1) resonance-enhanced multiphonon ionization. It was noted that the HCl alignment oscillates much faster in time than that of HF because of a stronger nuclear spin–rotation interaction and the additional nuclear electric quadrupole interaction. Similar calculations of the depolarization coefficient for HCl were carried out, which are consistent with the experimental data.[35]

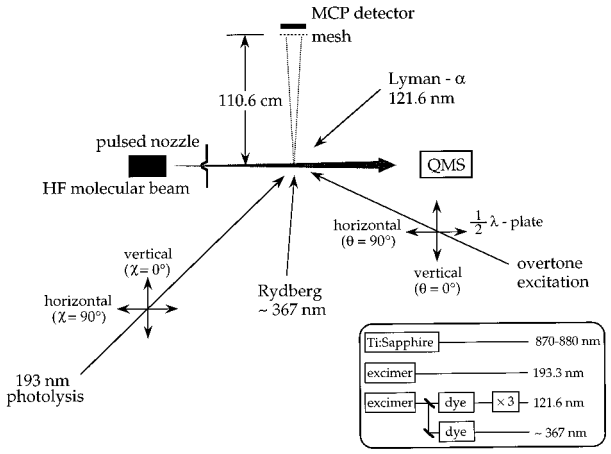

FIG. 1. Schematic of experimental arrangement.

The dependence of the H atom angular distribution on IR laser polarization indicated a pronounced alignment, whose time dependence was examined by varying the delay between the IR and UV lasers. Thus, we report HF($v=3$) alignment parameters as well as the first experimental demonstration of alignment depolarization in this system.

II. EXPERIMENT

The high-*n* Rydberg time-of-flight (HRTOF) technique has been applied to the H atom product to obtain center-of-mass (c.m.) translational energy distributions.[36] Our experimental setup has been described previously,[37] and a schematic is shown in Fig. 1. A pulsed molecular beam was produced by expanding typically 5% HF (99.99% wt.%, Matheson) in He or Ar at a total pressure of 760 Torr. Mixtures were expanded into the source chamber through a 0.75 mm diameter pulsed nozzle (General Valve, Series-9) operating at 10 Hz with a 400 μs pulse width. The molecular beam was differentially pumped and collimated by a 1 mm diameter skimmer located 2 cm from the nozzle. The molecular beam was crossed with the IR laser and photolysis laser beams 5 cm further downstream.

The scheme for the IR+UV photodissociation of HF is shown in Fig. 2. HF expanded in the pulsed molecular beam was first excited to a single rotational state of the $v=3$ level through an overtone transition.[38] This step was achieved by using a pulsed Ti:sapphire laser (STI, HRL100Z, 870–880 nm, 5–15 mJ, 500 MHz linewidth). The IR beam was fo-

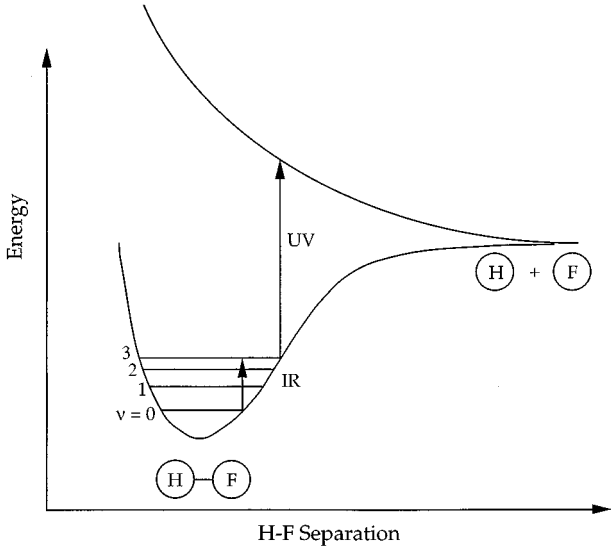

FIG. 2. IR+UV photodissociation scheme of HF molecule. Details of the excited surfaces are not shown.

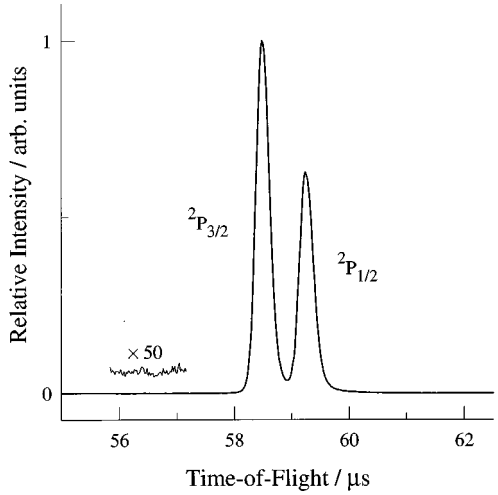

FIG. 3. H atom TOF spectrum of HF in $v=3$, $J=1$. 5% HF/Ar, total stagnation pressure 760 Torr, 6000 laser shots, $R(0)$ transition, vertical IR laser polarization, and unpolarized UV radiation (see Fig. 1 for definition).

cused with a 100 cm f.l. quartz lens. The linear polarization is nearly pure and was rotated by a half-wave plate (Newport). Due to the large HF overtone absorption cross section[39] and the narrow-linewidth IR laser output, second overtone excitation is efficient and it was possible to achieve excitation efficiencies as high as 10%–50%. However, saturation was avoided in our experiments. The parallel IR transitions, $R(0)$, $R(1)$, and $P(1)$ were utilized in this study. Photoacoustic spectra and a pulsed wavemeter (Burleigh, WA-4500) were used to match the Ti:sapphire laser frequency to the HF overtone transitions.

Vibrationally excited molecules were further excited with 193.3 nm radiation from an ArF excimer laser (Lambda Physik, EMG 101 MSC, 5–15 mJ directed into the vacuum chamber). The excimer laser beam was focused with a 65 cm f.l. quartz lens. This radiation could be polarized with an 8-plate stack of quartz slides placed at the Brewster angle, resulting in approximately 90% polarization. Hydrogen atoms produced from photodissociation were excited by 121.6 nm VUV radiation to the $2\,^2P$ state. This radiation was generated by tripling the 364.7 nm output from an excimer pumped dye laser (Lambda-Physik 3002) in Kr, and was focused in the interaction region by a MgF_2 lens. Another excimer pumped dye laser (Lambda-Physik 2001) further excited the H atoms from the $2\,^2P$ level to a high-n Rydberg level ($n=40$–90). The high-n Rydberg states are radiatively metastable and remain highly excited for many tens of microseconds. A small percentage of these excited atoms drift with their nascent velocities to a multichannel plate (MCP) detector (Galileo Electro-Optics), where they are detected as ions after being efficiently field ionized in front of the MCP. The flight path is 110.6 cm. TOF spectra were recorded by using a transient digitizer (DSP 2001) and averaged and stored in a computer. The sampling interval of the transient digitizer was 20 ns and typically 1000 channels around the region of interest were recorded; spectra usually represent 1–6×10^3 laser firings. In order to survey HF overtone spectra from the molecular beam, action spectra were also taken, i.e., intensities of integrated H atom TOF spectra from the IR+UV photodissociation were monitored as a function of IR laser wavelength. For the simple case of diatomic HF, action spectra are a direct reflection of the overtone absorption spectra. A similar technique to obtain overtone spectra has been reported.[40]

A less complex experiment was the VUV photodissociation of HF, as neither the IR laser nor the excimer photolysis laser were involved. The 121.6 nm VUV radiation served as both the photolysis source and probe radiation; 3.5×10^4 laser firings were required because of the weak VUV radiation.

III. RESULTS AND ANALYSIS

A. Spin–orbit branching ratio [F($^2P_{1/2}$)]/[F($^2P_{3/2}$)]

Shown in Fig. 3 is a TOF spectrum of the H atom product measured with optimized conditions and with the IR-laser-off background subtracted. The overtone transition is fixed on the $R(0)$ line, i.e., the IR excitation in the first step is $(v=3, J=1)\leftarrow(v=0, J=0)$. UV radiation induces dissociation of the HF molecules from $v=3$, $J=1$. Though the absorption cross section of HF at 193.3 nm is very small, the huge signal indicates a large enhancement of the absorption cross section after IR pre-excitation. H atoms deriving from one-photon UV and IR+UV two-photon excitation are well separated by the translational energy, and no signal from 193.3 nm radiation alone is observed. Note the excellent signal-to-noise ratio.

The c.m. translational energy spectrum shown in Fig. 4 is obtained from a direct conversion of the TOF spectrum in Fig. 3. Both the F($^2P_{1/2}$) spin–orbit energy and D_0(H–F) reflect the literature values.[41,42] The resolution, i.e., width of the peaks in Fig. 4, is limited by the excimer laser linewidth.

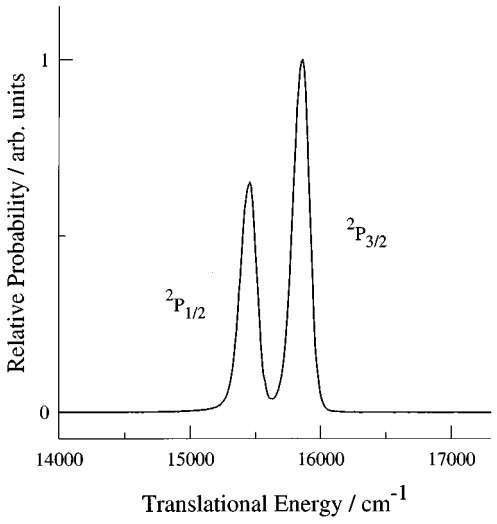

FIG. 4. c.m. translational energy distribution from direct conversion of the TOF spectrum in Fig. 3.

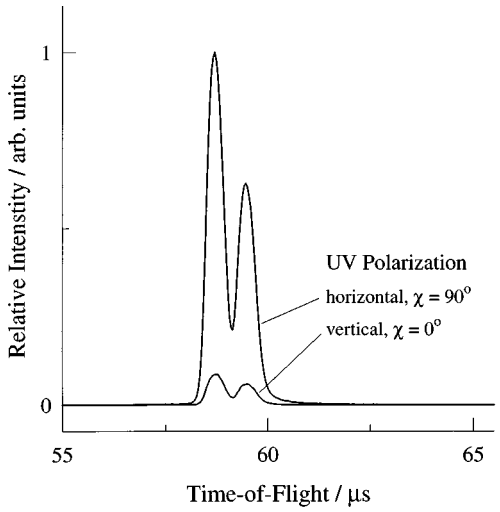

FIG. 5. UV polarization study: H atom TOF spectra of HF in $v=3$, $J=1$ with polarized UV radiation. IR laser polarization is vertical. $R(0)$ transition. Spectra are normalized to laser power and number of laser shots. Signals at vertical polarization are mainly due to imperfect polarization.

One must exercise care when determining the spin–orbit branching ratio $[F(^2P_{1/2})]/[F(^2P_{3/2})]$ in the IR+UV photodissociation experiment. In typical one-photon, electric-dipole-allowed photodissociation, sample molecules are initially randomly oriented in space, and the photofragment angular distribution can be described by[43]

$$I(\chi,\phi)=\frac{\sigma}{4\pi}[1+\beta P_2(\cos\chi)], \tag{3}$$

where β $(-1\leqslant\beta\leqslant 2)$ is the asymmetry parameter, χ is the polar angle between the electric vector of the polarized radiation and the final photofragment recoil direction, and ϕ is the azimuthal angle around the electric vector. In the case of IR+UV photodissociation, molecules are initially aligned by IR excitation before subsequent UV photodissociation, so initial molecular alignment must be taken into account. Hyperfine interaction will reduce the degree of alignment, as discussed later. For prompt photodissociation and axial recoil, the fragment angular distribution for an aligned molecule is given by[44]

$$I(\chi,\phi)=\frac{\sigma}{4\pi}P'_J(\chi,\phi)[1+\beta P_2(\cos\chi)]. \tag{4}$$

Note that in both Eqs. (3) and (4), χ is defined as the polar angle between the UV radiation polarization vector and the photofragment velocity or the detection direction (i.e., for fast dissociation, the angle between the UV radiation polarization vector and the molecular axis), and ϕ is the azimuthal angle around the UV polarization. $P'_J(\chi,\phi)$ is the probability of finding the molecule in the rotational state J with the molecular axis aligned at angles (χ,ϕ) with respect to the *UV laser polarization vector*. $P'_J(\chi,\phi)$ depends on the angle θ of the IR polarization and the detection direction, i.e., the molecular axis, and is described by Eq. (1). For special cases, simplified formulas can be derived from Eq. (4). For example, when the IR and UV polarization vectors are parallel, i.e., when $\theta=\chi$:

$$I(\chi)\propto[1+A_0(J)P_2(\cos\chi)][1+\beta P_2(\cos\chi)]. \tag{5}$$

On the other hand, when the electric vectors of the IR and UV radiations are perpendicular to each other and the photofragment is detected *in the plane of the two electric vectors*, $\theta=90°-\chi$. In this case, the angular distribution is given by

$$I(\chi)\propto[1+A_0(J)P_2(\cos(90°-\chi))][1+\beta P_2(\cos\chi)]. \tag{6}$$

In the H fragment TOF distribution measurement shown in Fig. 5, the IR polarization is along the flight path. With horizontally and vertically polarized UV (see Fig. 1), the angles χ between the UV polarization and the flight path are 90° and 0°, respectively. Since the detector solid angle is small, the terms for the probabilities of HF alignment in both situations become identical, i.e., $[1+A_0(J)P_2(\cos 0°)]$. Therefore, at these two specific angles, the relative H fragment angular distribution can be reduced to Eq. (3).

It is clear from Fig. 5 that when the UV laser is horizontally polarized, i.e., perpendicular to the flight path, the H atom signal is a maximum, whereas the signal with the UV polarization parallel to the flight path is a minimum. The signal observed with vertically polarized UV radiation is a result of imperfect polarization from the stacked quartz-plate polarizer. Since HF is aligned along the flight path (IR polarization along the flight path and the $R(0)$ transition), it is obvious that the electronic transition dipole moment of HF is perpendicular to its molecular axis. The peaks associated with both F* and F appear to have the same UV polarization dependence. In order to obtain β parameters for the two channels, relative intensities of the two peaks at different UV polarizations must be used. The two F atom peaks are fitted

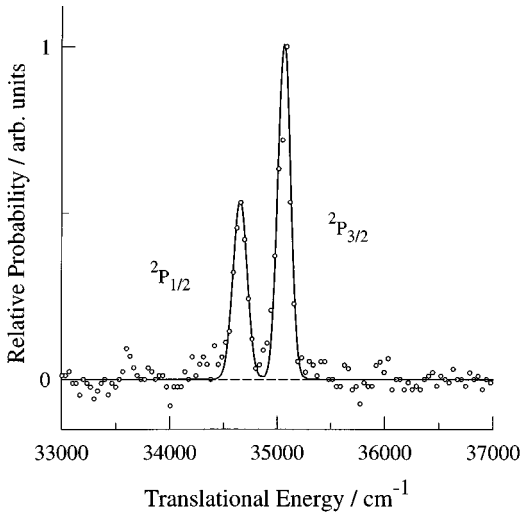

FIG. 6. c.m. translational energy distribution of HF photodissociation at 121.6 nm. 5% HF/Ar and 760 Torr total stagnation pressure. Circles are from direct conversion of experimental TOF spectrum, while the solid line represents the fit using Gaussian functions.

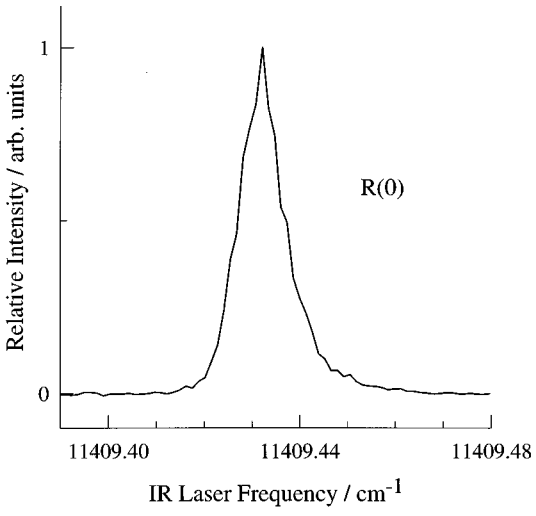

FIG. 7. H atom product action spectrum: total H atom yield is monitored with the IR laser scanned across the $R(0)$ transition line. The linewidth is mainly from the laser linewidth.

to Gaussian or Voigt functions and the areas of the peaks are used. Correction for imperfect polarization is also taken into account. The resulting β parameters for the two product channels are estimated to be: $\beta(F^*)=-1.0\pm0.05$ and $\beta(F)=-1.0\pm0.05$. Thus, it appears that both channels derive from the perpendicular transition $A\ ^1\Pi\leftarrow X\ ^1\Sigma^+$. Since both channels have the same β, calculation of the spin-orbit branching ratio F*/F is trivial; the ratio of the peaks in the c.m. translational energy distribution directly reflects the spin–orbit branching ratio. Our best estimate is $[F(^2P_{1/2})]/[F(^2P_{3/2})]=0.71\pm0.03$.

Photodissociation at 121.6 nm has also been observed. The c.m. translational energy distribution from direct conversion of the TOF spectrum is shown in Fig. 6. The VUV linewidth is sufficiently narrow ($\sim$1 cm^{-1}) to ensure that the peak width reflects the TOF spectrometer resolution. Because of the noise in the distribution, the peaks are fitted with Gaussian functions and relative areas are used to obtain the branching ratio. Though the VUV radiation is mainly vertically polarized, we were unable to conduct a VUV polarization study due to the low signal intensity. Since $A\ ^1\Pi\leftarrow X\ ^1\Sigma^+$ is likely to be the only electronic transition at 121.6 nm,[22–26] it is reasonable to assume that both channels have the same β. In this case, the relative areas of the two channels indicate a spin–orbit branching ratio of 0.69 ± 0.14.

B. H atom action spectra

Overtone spectra have often been recorded by using photoacoustic spectroscopy because of its high sensitivity. Since this is usually done with a room temperature sample, resolution is affected by spectral congestion, pressure broadening and Doppler broadening. Though these drawbacks can be overcome by using a supersonic jet instead of a gas cell, a sensitive technique is required. Spectroscopic techniques such as intracavity laser absorption spectroscopy (ICLAS),[45] ion dip spectroscopy,[46] and optothermal spectroscopy,[47] have been used with supersonic beams. Photofragment spectroscopy is another common technique for studying overtone spectroscopy. For example, multiphoton infrared laser assisted photofragment spectroscopy (IRLAPS) with LIF detection,[48] vibrationally mediated UV photodissociation with LIF detection,[49] and vibrationally mediated UV photodissociation with multiphonon ionization detection[40] have been demonstrated as effective tools to study overtone spectroscopy of molecular beam samples.

Our approach is similar to the last two techniques. The total integrated intensities of the H photofragment are recorded as the IR laser is scanned through an overtone transition. The action spectra of the H atom product are effectively the HF overtone spectra. This technique mass selects the H atom with the advantage that space charge effects due to ionization are avoided. A typical scan over the $R(0)$ transition in the second overtone band is shown in Fig. 7. The linewidth is measured to be $\sim$0.01 cm^{-1}, which is the convolution of the laser linewidth and residual Doppler width of the HF molecules in a supersonic jet. Care was taken to avoid saturation of the transition. Almost identical action spectra were taken with both HF/Ar and HF/He mixtures, indicating minimal Doppler broadening. The measured peak width is consistent with the linewidth of the Ti:sapphire laser, and the peak position is within the accuracy of the wavemeter.

C. Alignment parameters and depolarization coefficient

Since HF photodissociation is prompt, the H fragment will travel in the direction of the HF axis. The experimental geometry (Fig. 1) is such that if HF is initially aligned, the angular distribution using unpolarized UV will only depend on the IR polarization direction, and therefore can be used to measure the IR alignment parameter. The dependence of the

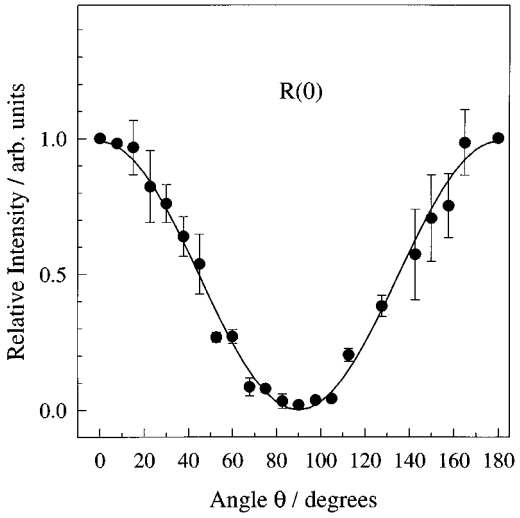

FIG. 8. Measurement of alignment parameter for $R(0)$ transition: total intensity of H atom product vs IR polarization. Filled dots are experimental measurements, normalized to that at $\theta=0°$, i.e., when the IR polarization and the flight path are parallel. The solid line is a fit using Eq. (1), giving a $\cos^2\theta$ distribution, i.e., an alignment parameter of 2.0 ± 0.1.

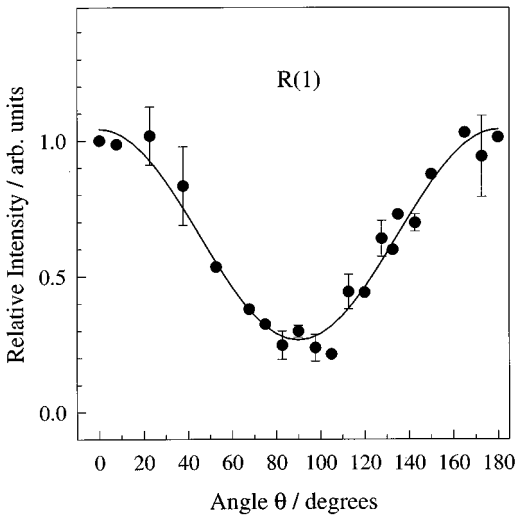

FIG. 9. Same as in Fig. 8, but for the $R(1)$ transition. The alignment parameter is 1.0 ± 0.1.

H atom TOF intensities can be described by Eq. (1). Note that θ in Eq. (1) is the angle between the IR polarization direction and the flight path.

Figure 8 shows the intensities of integrated H atom TOF spectra for the $R(0)$ transition at various IR polarization angles with respect to the flight path. The IR polarization was rotated by using a half-wave plate. To minimize depolarization due to hyperfine interaction, the TOF spectra were taken with minimum delay between the IR laser pulse and the UV photolysis laser pulse. Because of the small but finite solid angle of the detector and the large ratio between the H atom c.m. velocity and the parent molecule lab velocity, correction for the angular distribution due to a lab→c.m. system transform is negligible. In order to minimize changes in experimental conditions such as IR laser frequency drift, laser power fluctuation, etc., a reference angle of $\theta=0°$ was chosen. Reference TOF spectra were taken for every 2–3 TOF spectra at other angles and each TOF spectrum was accumulated from 500 laser shots. The dots in Fig. 8 are the experimental data normalized to the reference angle, and the error bars derive principally from the wavelength fluctuation of the IR laser. The solid line is from a least-squares fit using Eq. (1). The alignment parameter $A_0^R(0)$ is estimated to be 2.0 ± 0.1, in agreement with the theoretical value.[27,32] For $R(0)$, the probability of HF alignment along the IR polarization vector is indeed a $\cos^2\theta$ distribution.

A similar experiment was carried out for $R(1)$ and the results are given in Fig. 9. The best fit for $A_0^R(1)$ is 1.0 ± 0.1, in agreement with the theoretical value.[27,32] For $P(1)$, the molecular axes are distributed isotropically, i.e., $A_0^P(1)=0$.[27,32] The data in Fig. 10 verify this.

The time-dependence of the alignment parameter can be measured by varying the delay between the IR and UV lasers, as in the study of Orr-Ewing *et al.*[35] Measurements of the H atom signal intensities with the IR laser horizontally and vertically polarized allow us to calculate the alignment parameter by using Eq. (1). The half-wave plate was rotated to achieve horizontal and vertical polarization alternatively at each delay. There is a practical limit to the delay, since HF($v=3$) molecules move out of the UV laser probe region as per the beam velocity. The weak hyperfine interaction gives $\sim\mu$s recurrence times, which are readily observed in an HF/Ar beam. Though the absolute signal intensity drops as the delay increases, the alignment parameter depends only on a ratio of signal intensities. In the present study, $R(0)$ was chosen since it undergoes the largest degree of depolarization.[28,33] The depolarization coefficient $G^{(2)}(t)$ was obtained from the measured alignment parameters $A_0(t)$ by using Eq. (2). Note that for $R(0)$, $A_0(t=0)$ is 2. The filled

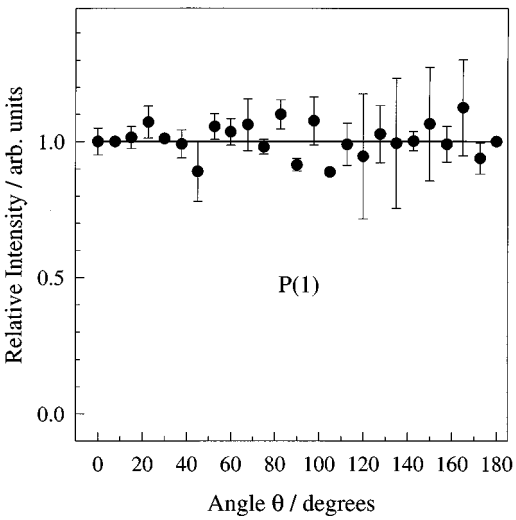

FIG. 10. Same as in Fig. 8, but for the $P(1)$ transition. The alignment parameter is 0, corresponding to an isotropic distribution.

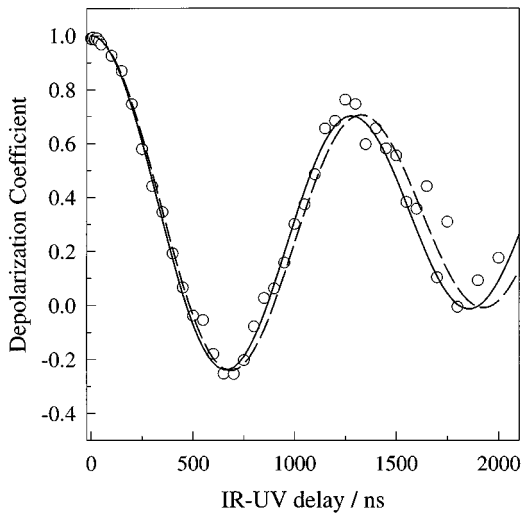

FIG. 11. Depolarization coefficient as a function of IR–UV delay. Dashed and solid lines are calculations; see text for details.

dots in Fig. 11 show the measured depolarization coefficient for various delays, and a pronounced oscillation is observed. A comparison between experimental results and theoretical calculations is presented below.

IV. DISCUSSION

A. Photodissociation mechanisms and spin–orbit branching ratio

The $X\ ^1\Sigma^+$ ground state correlates adiabatically with $H(^2S)+F(^2P_{3/2})$. Among the excited states, $A\ ^1\Pi$, $a\ ^3\Pi_2$, $a\ ^3\Pi_1$, and $a\ ^3\Pi_{0-}$ correlate adiabatically with $H(^2S)+F(^2P_{3/2})$, while $1\ ^3\Sigma^+$ and $a\ ^3\Pi_{0+}$ correlate adiabatically with $H(^2S)+F(^2P_{1/2})$.[7,9,12] Since singlet–triplet transitions are negligible for a small molecule like HF,[9] the only allowed transition in the region of the first absorption is $A\ ^1\Pi \leftarrow X\ ^1\Sigma^+$, consistent with the perpendicular nature of this channel.

Since both spin–orbit channels have the same UV polarization dependence (and thus the same β), they both probably derive from the $A\ ^1\Pi$ state which is accessed in the Franck–Condon region. It is the couplings at large separation that determine the spin–orbit branching ratio. Unlike HI, since the UV photoexcitation of HF is restricted to singlet–singlet transitions, there is no complication from initial population of multiple electronic states. In the adiabatic limit, the atoms separate slowly and the initially populated molecular states correlate adiabatically with the atomic fragment spin–orbit states, i.e., the branching ratio $[^2P_{1/2}]/[^2P_{3/2}]$ for HF should be 0. In the diabatic limit, separation occurs very fast such that the formation probabilities of $^2P_{1/2}$ and $^2P_{3/2}$ are determined by the probabilities of projecting the molecular wave function onto the eigenstates of the separated atoms. The branching ratio $[^2P_{1/2}]/[^2P_{3/2}]$ in the diabatic limit is 0.5.[7,50] Our measurement of the branching ratio in IR+UV photodissociation shows that $[F(^2P_{1/2})]/[F(^2P_{3/2})]=0.71\pm0.03$. This corresponds to neither the adiabatic limit nor the diabatic limit, being higher than both. Even for 121.6 nm photodissociation, the diabatic limit is not achieved.

Detailed theoretical studies of HCl have helped elucidate its photodissociation mechanisms,[8–11] and this knowledge is also applicable to HF. At large H–F distances where the spin–orbit energy becomes significant, couplings of $A\ ^1\Pi$ and neighboring triplets will redistribute the photodissociation flux and thus determine the product spin–orbit branching ratio. Spin–orbit coupling between $A\ ^1\Pi$ and the $\Omega=1$ components of $a\ ^3\Pi$ and $1\ ^3\Sigma^+$ may play an important role. As with HCl,[2–11] dissociation cannot be assigned to either the adiabatic or diabatic limit. A complex spin–orbit coupling of the excited potential curves is involved, and we hope this work will stimulate a theoretical study of the HF spin–orbit branching ratio.

B. Alignment and depolarization

Though the optical pulse aligns the rotational angular momentum of the molecule with $A_0(t=0)$, coupling of the rotational angular momentum and the nuclear spin will subsequently reduce the degree of alignment. Note that in our experiment we measure the alignment of the molecular axis instead of the rotational angular momentum. However, these two alignment parameters exhibit the same time dependence and they are directly related. $A_0(t)$ evolves in time as per Eq. (2), which defines the time-dependent depolarization coefficient, $G^{(2)}(t)$. For a diatom with a single spin this is given by Blum[31] and Zare:[32]

$$G^{(k)}(t)=\sum_{F,F'}\frac{(2F'+1)(2F+1)}{(2I+1)}\times\begin{Bmatrix}F' & F & k\\ J & J & I\end{Bmatrix}^2\cos[(E_{F'}-E_F)t/\hbar], \tag{7}$$

where k is the order of orientation and alignment parameters and E_F and $E_{F'}$ are energy levels from coupling of rotational and nuclear spin angular momenta.

The depolarization coefficient of a molecule with two nuclear spins, I_1 and I_2 has been derived by Fano and Macek[30] and by Altkorn, Zare, and Greene:[33]

$$G^{(k)}(t)=\frac{1}{(2I_1+1)(2I_2+1)}\sum_{\substack{\alpha,\alpha'\\F,F'}}(2F'+1)(2F+1)\times\left|\sum_{F_i,F_i'}(-1)^{F_i+F_i'}[(2F_i+1)(2F_i'+1)]^{1/2}\times c^{(F)}_{\alpha F_i}c^{(F')*}_{\alpha' F_i'}\begin{Bmatrix}F_i' & F' & I_2\\ F & F_i & k\end{Bmatrix}\times\begin{Bmatrix}J & F_i' & I_1\\ F_i & J & k\end{Bmatrix}\right|^2\cos[(E_{\alpha F}-E_{\alpha' F'})t/\hbar]. \tag{8}$$

Calculation of the depolarization coefficient has been described extensively by Altkorn and co-workers[33] and Orr-Ewing and co-workers,[35] and their computer program has

been used here. In the present study, HF($v=3$) is examined, whereas previous studies were limited to $v=0$ and 1.[51–55] Since hyperfine coupling constants for HF($v=3$) are unavailable from experiment, they must be estimated. A comparison of the calculated depolarization coefficient using the estimated constants can provide insight into the vibrational and rotational dependence of these constants at higher vibrational states.

Hyperfine interaction in HF is represented by the Hamiltonian:[51,53]

$$H=C_{\mathrm{F}}(\mathbf{I_F}\cdot\mathbf{J})+C_{\mathrm{H}}(\mathbf{I_H}\cdot\mathbf{J})+J_{\mathrm{HF}}(\mathbf{I_H}\cdot\mathbf{I_F})+5S_{\mathrm{HF}} \times\frac{3(\mathbf{I_F}\cdot\mathbf{J})(\mathbf{I_H}\cdot\mathbf{J})+3(\mathbf{I_H}\cdot\mathbf{J})(\mathbf{I_F}\cdot\mathbf{J})-2(\mathbf{I_F}\cdot\mathbf{I_H})J(J+1)}{(2J+3)(2J-1)}, \tag{9}$$

where C_{F} and C_{H} are spin–rotation constants, J_{HF} is the indirect (electron-coupled) spin–spin interaction constant, and S_{HF} is the direct spin–spin interaction constant. These hyperfine constants define the energy levels whose splittings determine the recurrence times, as shown in Eq. (8).

It is known that hyperfine constants depend on vibrational and rotational states via their dependence on internuclear distance,[51–55] and that they can be expanded in a Taylor series about the equilibrium internuclear distance R_e:

$$\langle C\rangle_{vJ}=C_e+\left.\frac{dC}{d\xi}\right|_{R_e}\langle\xi\rangle_{vJ}+\left.\frac{1}{2}\frac{d^2C}{d\xi^2}\right|_{R_e}\langle\xi^2\rangle_{vJ}+\cdots, \tag{10}$$

where $\xi=(R-R_e)/R_e$. In previous studies,[51,53,55] the vibration–rotation expectation values of ξ with only the linear vibrational term were considered, resulting in a simple semiquantitative model for HF:[53] $C_{vJ}=C(v,J=0)+av+bJ(J+1)$. The fluorine and hydrogen spin–rotation constants C_{F} and C_{H} increase with vibrational and rotational quantum numbers, while the direct spin–spin constant S_{HF} decreases slowly with increasing quantum numbers. The C_{F} constant is predominant among the hyperfine constants and is sensitive to the change in vibrational and rotational states. The hyperfine structure constants can be extrapolated using this semiquantitative formula,[53] and the corresponding calculation of the depolarization coefficient is shown by the dashed line in Fig. 11. However, a more accurate evaluation of the expectation values has been proposed,[55] in which contributions from quadratic terms in vibration are included, especially at higher vibrational levels. Using the accurate analytic forms of the expectation values[56] and the derivatives of the constants,[55] we estimated the $v=3$, $J=1$ hyperfine constants: $C_{31}(\mathrm{F})=483$ kHz, $C_{31}(\mathrm{H})=-66$ kHz, $S_{31}(\mathrm{HF})=139$ kHz. The indirect spin–spin coupling constant is very small and the value for the ground state (0.529 kHz) is used. Compared to the well-known ground state values: $C_{01}(\mathrm{F})=307.65$ kHz, $C_{01}(\mathrm{H})=-71.10$ kHz, $S_{01}(\mathrm{HF})=143.45$ kHz, there is a significant increase in the C_{F} constant, as expected. The calculation for the depolarization of $v=3$, $J=1$ using this new set of constants is shown as the solid line in Fig. 11. Agreement with the data is excellent, supporting the extrapolated hyperfine constants.

The depolarization coefficient $G^{(2)}(t)$ for $R(0)$ ($v=3$, $J=1$) oscillates and does not return to the initial value of unity during our measurement time. In this short time frame, the first recurrence corresponds to the fastest beat frequency, i.e., the largest energy splitting in the hyperfine levels. The measured frequency in this experiment is most sensitive to C_{F}, and the values used for the two calculations differs by about 15 kHz. Both calculated depolarization coefficients are close to the data, but close inspection favors the solid curve using the set of improved hyperfine constants.[55,56] Data at large delays are noisy due to the decreased signal intensity. However, data in the high signal-to-noise region (delays <1.5 μs) agree best with the solid line, suggesting a contribution from higher order terms in vibration. Similar behavior has been observed in HCl.[57]

V. SUMMARY

This study has expanded the experimental database concerning HF photophysics. Dissociation is photoinitiated from a single $v=3$ rotational state, and UV polarization studies indicate that the transition dipole moment is perpendicular to the molecular axis ($A\ ^1\Pi\leftarrow X\ ^1\Sigma^+$) and F^* and F peaks both have the same β parameters. The branching ratio was measured for both the IR+UV ($F^*/F=0.71\pm0.03$) and VUV ($F^*/F=0.69\pm0.14$) photolysis schemes, which corresponds to neither the adiabatic nor diabatic limits.

For unpolarized UV, the angular recoil distribution of photofragments depends on the orientation of the electric vector of the linearly polarized IR radiation, thus manifesting the IR alignment effect. Several alignment parameters were determined: $A_0^R(0)=2.0\pm0.1$, $A_0^R(1)=1.0\pm0.1$, $A_0^P(1)=0$, in agreement with theory.

Time dependence of the alignment parameter was measured by varying the delay between the IR and UV lasers. For $R(0)$, a strong oscillation of the alignment parameter was observed with $\sim\mu$s recurrence time. The hyperfine coupling of HF in $v=3$ was examined, testing the vibrational dependence of the coupling constants. Contributions from higher order terms in vibration are suggested.

ACKNOWLEDGMENTS

We thank Professor Zare and Dr. Simpson and Dr. Orr-Ewing for sending their depolarization coefficient program and a reprint. C.W.R. thanks the Deutsche Forschungsgemeinschaft for a scholarship. This work was supported by the U.S. Department of Energy (Grant No. DE-FG03-85 ER13363).

[1] (a) R. S. Mulliken, J. Chem. Phys. **3**, 506 (1935); (b) R. S. Mulliken, Phys. Rev. **51**, 310 (1937); (c) R. S. Mulliken, J. Chem. Phys. **8**, 382 (1940).
[2] E. Tiemann, H. Kanamori, and E. Hirota, J. Chem. Phys. **88**, 2457 (1988).
[3] Y. Matsumi, P. K. Das, and M. Kawasaki, J. Chem. Phys. **92**, 1696 (1990).
[4] Y. Matsumi, K. Tonokura, M. Kawasaki, and T. Ibuki, J. Chem. Phys. **93**, 7981 (1990).
[5] J. Park, Y. Lee, and G. W. Flynn, Chem. Phys. Lett. **186**, 441 (1991); **192**, 138 (1992).
[6] (a) Y. Matsumi, P. K. Das, M. Kawasaki, K. Tonokura, T. Ibuki, G. Inoue, S. Satyapal, and R. Bersohn, J. Chem. Phys. **97**, 5261 (1992); (b) K.

Tonokura, Y. Matsumi, M. Kawasaki, S. Tasaki, and R. Bersohn, *ibid*. **97**, 8210 (1992).
[7] R. Liyanage, Y. Yang, S. Hashimoto, R. J. Gordon, and R. W. Field, J. Chem. Phys. **103**, 6811 (1995).
[8] S. C. Givertz and G. G. Balint-Kurti, J. Chem. Soc. Faraday Trans. **82**, 1231 (1986).
[9] M. H. Alexander, B. Pouilly, and T. Duhoo, J. Chem. Phys. **99**, 1752 (1993).
[10] I. H. Gersonde, S. Hennig, and H. Gabriel, J. Chem. Phys. **101**, 9558 (1994).
[11] T. Duhoo and B. Pouilly, J. Chem. Phys. **103**, 182 (1995).
[12] Z. Xu, B. Koplitz, and C. Wittig, J. Phys. Chem. **92**, 5518 (1988).
[13] T. Kinugawa and T. Arikawa, J. Chem. Phys. **96**, 4801 (1992).
[14] R. D. Clear, S. J. Riley, and K. R. Wilson, J. Chem. Phys. **63**, 1340 (1975).
[15] R. Schmiedl, H. Dugan, W. Meier, and K. H. Welge, Z. Phys. A **304**, 137 (1982).
[16] G. N. A. Van Veen, K. A. Mohamed, T. Baller and A. E. De Vries, Chem. Phys. **80**, 113 (1983).
[17] I. Levy and M. Shapiro, J. Chem. Phys. **89**, 2900 (1988).
[18] P. F. Zittel and D. D. Little, J. Chem. Phys. **71**, 713 (1979).
[19] C. Kalyanaraman and N. Sathyamurthy, Chem. Phys. Lett. **209**, 52 (1993).
[20] E. Safary, J. Romand, and B. Vodar, J. Chem. Phys. **19**, 379 (1951).
[21] J. B. Nee, M. Suto, and L. C. Lee, J. Phys. B **18**, L293 (1985).
[22] C. F. Bender and E. R. Davidson, J. Chem. Phys. **49**, 4989 (1968).
[23] T. H. Dunning, Jr., J. Chem. Phys. **65**, 3854 (1976).
[24] G. A. Segal and K. Wolf, Chem. Phys. **56**, 321 (1981).
[25] M. Bettendorff, R. J. Buenker, S. D. Peyerimhoff, and J. Römelt, Z. Phys. A **304**, 125 (1982).
[26] A. P. Hitchcock, G. R. J. Williams, C. E. Brion, and P. W. Langhoff, Chem. Phys. **88**, 65 (1984).
[27] R. N. Zare, Ber. Bunsenges. Phys. Chem. **86**, 422 (1982).
[28] C. H. Greene and R. N. Zare, Annu. Rev. Phys. Chem. **33**, 119 (1982).
[29] K. Bergmann, in *Atomic and Molecular Beam Methods Volume 1*, edited by G. Scoles (Oxford U.P., New York, 1988).
[30] U. Fano and J. H. Macek, Rev. Mod. Phys. **45**, 553 (1973).
[31] K. Blum, *Density Matrix Theory and Applications* (Plenum, New York, 1981).
[32] R. N. Zare, *Angular Momentum. Understanding Spatial Aspects in Chemistry and Physics* (Wiley Interscience, New York, 1988).
[33] R. Altkorn, R. N. Zare, and C. H. Greene, Mol. Phys. **55**, 1 (1985).
[34] C. Yan and A. C. Kummel, J. Chem. Phys. **98**, 6869 (1993).
[35] A. J. Orr-Ewing, W. R. Simpson, T. P. Rakitzis, and R. N. Zare, Israel J. Chem. **34**, 95 (1994).
[36] L. Schneider, W. Meier, K. H. Welge, M. N. R. Ashfold, and C. Western, J. Chem. Phys. **92**, 7027 (1990).
[37] (a) J. Segall, Y. Wen, R. Lavi, R. Singer, and C. Wittig, J. Phys. Chem. **95**, 8078 (1991); (b) J. Zhang, C. W. Riehn, M. Dulligan, and C. Wittig, J. Chem. Phys. **103**, 6815 (1995).
[38] (a) D. E. Mann, B. A. Thrush, D. R. Lide, Jr., J. J. Ball, and N. Acquista, J. Chem. Phys. **34**, 420 (1961); (b) E. S. Fishburne and K. Narahari Rao, J. Mol. Spectrosc. **19**, 290 (1966); (c) H. Sasada, *ibid.* **165**, 588 (1994).
[39] R. L. Spellicy, R. E. Meredith, and F. G. Smith, J. Chem. Phys. **57**, 5119 (1972).
[40] (a) M. Hippler and M. Quack, Chem. Phys. Lett. **231**, 75 (1994); (b) M. Hippler and M. Quack, Ber. Bunsenges. Phys. Chem. **99**, 417 (1995).
[41] C. E. Moore, *Atomic Energy Levels*, National Stand. Ref. Data Ser., National Bureau of Standards, Washington DC, 1971.
[42] K. P. Huber and G. Herzberg, *Molecular Spectra and Molecular Structure IV. Constants of Diatomic Molecules* (Van Nostrand, New York, 1979).
[43] R. N. Zare, Mol. Photochem. **4**, 1 (1972).
[44] (a) S. E. Choi and R. B. Bernstein, J. Chem. Phys. **85**, 150 (1986); (b) R. N. Zare, Chem. Phys. Lett. **156**, 1 (1989); (c) C. A. Taatjes, M. H. M. Janssen, and S. Stolte, *ibid.* **203**, 363 (1993). The formula for alignment can be readily derived from these references.
[45] A. Campargue, F. Stoeckel, and M. Chenevier, Spectr. Acta. Rev. **13**, 69 (1990).
[46] R. H. Page, Y. R. Shen, and Y. T. Lee, Phys. Rev. Lett. **59**, 1293 (1987).
[47] T. E. Gough, R. E. Miller, and G. Scoles, Appl. Phys. Lett. **30**, 338 (1977).
[48] R. D. F. Settle and T. R. Rizzo, J. Chem. Phys. **97**, 2823 (1992).
[49] L. J. Butler, T. M. Ticich, M. D. Likar, and F. F. Crim, J. Chem. Phys. **85**, 2331 (1986).
[50] S. J. Singer, K. F. Freed, and Y. B. Band, Adv. Chem. Phys. **61**, 1 (1985).
[51] J. S. Muenter and W. Klemperer, J. Chem. Phys. **52**, 6033 (1970).
[52] J. S. Muenter, J. Chem. Phys. **56**, 5409 (1972).
[53] C. Breant, T. Baer, D. Nesbitt, and J. L. Hall, *Sixth International Conference on Laser Spectroscopy* (Springer, New York, 1983), Vol. 138.
[54] D. K. Hindermann and C. D. Cornwell, J. Chem. Phys. **48**, 4148 (1968).
[55] S. M. Bass, R. L. Deleon, and J. S. Muenter, J. Chem. Phys. **86**, 4305 (1987).
[56] R. H. Tipping and J. F. Ogilvie, J. Mol. Struct. **35**, 1 (1976).
[57] E. W. Kaiser, J. Chem. Phys. **53**, 1686 (1969).